Thermal Shock and Thermal Fatigue Behaviour of Si$_3$N$_4$-Ceramics

G.A. Schneider, F. Magerl and G. Petzow

Max-Planck-Institut für Metallforschung, Institut für Werkstoffwissenschaft,
Pulvermetallurgisches Laboratorium
D-7000 Stuttgart 80, Germany

Crack propagation of radially oriented edge cracks in thermally loaded thin discs by lamp irradiation is used to study the thermal shock and thermal fatigue behaviour of Si$_3$N$_4$-ceramics. The sample temperature is measured by scanning the disc surface with an infrared pyrometer and used to calculate the stress intensity factor, K_I, as a function of the crack length. The crack growth is observed and recorded using a stereo-microscope connected to CCD-camera, giving a spatial resolution of approximately 5 μm. Stable and unstable crack as well as subcritical crack growth are observed unambiguously. Very short starter cracks allow the measurement of very steep R-curves in Si$_3$N$_4$. Subcritical crack growth under static and cyclic thermal loading is evaluated in terms of crack extension versus time curves and crack velocity versus K_I-curves. Some general consequences of these results concerning thermal shock applications of Si$_3$N$_4$ are discussed.

1. INTRODUCTION

The range of applications of ceramics at high temperatures often involves the occurrence of thermal stresses. The thermal loading of the material may be transient - the so called thermal shock - static (steady state), or cyclic, denoted as thermal cycling or thermal fatigue loading. Despite of the undisputed importance and the practical relevance of these loadings for the reliability of components there are very little quantitative fracture mechanical examinations of the crack propagation under pure thermal loading [1-9].

The objective of this paper is to present quantitative results for unstable and stable as well as subcritical crack propagation in Si$_3$N$_4$ under exclusively thermal loading conditions which are representative for thermal shock as well as thermal fatigue transient loadings. The results are discussed fracture mechanically with special emphasis on R-curve behavior and subcritical crack growth (SCG). The experiment was performed with a lamp irradiation apparatus as described in [10,11].

2. MATERIAL AND SAMPLE PREPARATION

A hot pressed Si$_3$N$_4$ (Fraunhofer-Establishment, IKTS, Dresden), SN84 (NGK, Japan) and postHIPed reaction bonded Si$_3$N$_4$ (HIPRBSN) were used. From the bulk material cylinders were drilled out and cut into 0.7mm thick disks. The disks were ground down to a final thickness of 0.2 to 0.3mm. One side was polished to a surface roughness of 6 μm. A 50μm thin saw blade was used to produce upto 4mm long radially oriented notches.

3. THERMAL LOADING

Thermal stresses are generated by irradiating the center of a circular disk. This causes a lateral, axi-symmetrically, quasi two-dimensional temperature field in the disc with much higher temperatures in the center of the disk than at the outer rim. Correspondingly tensile hoop stresses arise near the outer rim which are used to study the crack propagation of a radially oriented edge crack. The measured temperature field and crack elongation

allows detailed fracture mechanical analysis of the crack propagation in this model system.

3.1 Thermal Loading Cell

A 150W tungsten lamp situated in the focal point of an ellipsoidal gold coated mirror is used to irradiate one side of a ceramic disc (Fig. 1). The disks, with diameters from 11 - 15 mm and a thickness from 0.2 to 0.3 mm, are adjusted in the focal plane of the mirror of the tungsten lamp. In order to avoid external mechanical constraints, the disk is mounted by two diametrically placed soft-spring-loaded ZrO_2 pins. At full voltage, corresponding to 15 V, the lamp irradiation allows the immediate evaporation of Si_3N_4 corresponding to a temperature of approximately 1800 C. Maximum heating rates are approximately 1000 K/s.

3.2 Measurement and Control Unit

The whole measurement system is depicted in Fig. 2. An infrared pyrometer with a measurement spot size of 1 mm is used to detect the temperature on the non-irradiated back side of the disk. A stereo microscope coupled to a CCD-camera with monitor and recorder allows the in situ observation of crack growth with a spatial resolution of 5 μm. The whole system is mounted on an optical bench with positioning tables of a precision of 10 μm. The optical control with the stereo-microscope allows a reproducible positioning of the samples with an accuracy of 5 μm. The temperature measurement as well as the applied lamp voltage is computer controlled allowing almost arbitrary voltage profiles as a function of time.

3.3. Temperature and Stress Field

The experiments are run under quasi steady state conditions which means that the change in applied voltage is slow enough that steady state temperature profiles are present in the sample. Therefore the temperatures for different applied voltages varying from 2 to 10 V according the ceramic material were measured under steady state conditions. The sample surface is scanned horizontally and vertically in order to insure radial symmetry.

An even forth-order polynomial was used to describe the temperature field T(r,t). The data points were fitted with a Householder algorithm:

$$T(r,t) = a_0(t) + a_2(t) r^2 + a_4(t) r^4 \qquad (1)$$

The time dependent coefficients a_0, a_2 and a_4 are the fitting parameters, r denotes the radius, and t the time.

As an example Figure 3 shows the measured temperature fields for Si_3N_4 . In general differently produced Si_3N_4 materials show similar temperature profiles revealing similar heat capacities and thermal conductivities. The temperature profiles of the tested samples were flat enough to be reasonably fitted by a fourth order polynomial. Temperature gradients in thickness direction and corresponding bending moments can be neglected because of the very thin samples.

The thermal stresses corresponding to the temperature polynomial of eq. 1 are easily calculated [12]. For the hoop stresses $\sigma_{\theta\theta}$ the following result is found, R denoting the radius of the disk:

$$\sigma_{\theta\theta} = \alpha E\{ [(1/4)a_2 R^2 + (1/6)a_4 R^4]$$

$$-(3/4)a_2 r^2 - (5/6)a_4 r^4 \} \qquad (2)$$

The radial stresses are not discussed because of the radially oriented crack direction.

Because the thermal expansion coefficient and the Young's modulus are a function of temperature the material properties for the average temperature

$$T_a = (1/2) [T(r=0,t) + T(r=R,t)] \qquad (3)$$

were introduced in eq. 2 to calculate the stresses. Figure 4 shows the results of the tangential stress calculations for the Si_3N_4 material with the temperature distribution of Figure 3. For Si_3N_4 maximum tensile stresses of approximately 135 MPa are produced which are clearly below the bending strength of the material. In order to achieve steep enough temperature gradients to fracture Si_3N_4 discs Nd-YAG laser irradiation thermal shock equipments have been developed [13].

3.4 Stress Intensity Factor Calculation

Analytical and semi-analytical results for the stress intensity factors of radially oriented edge cracks of a
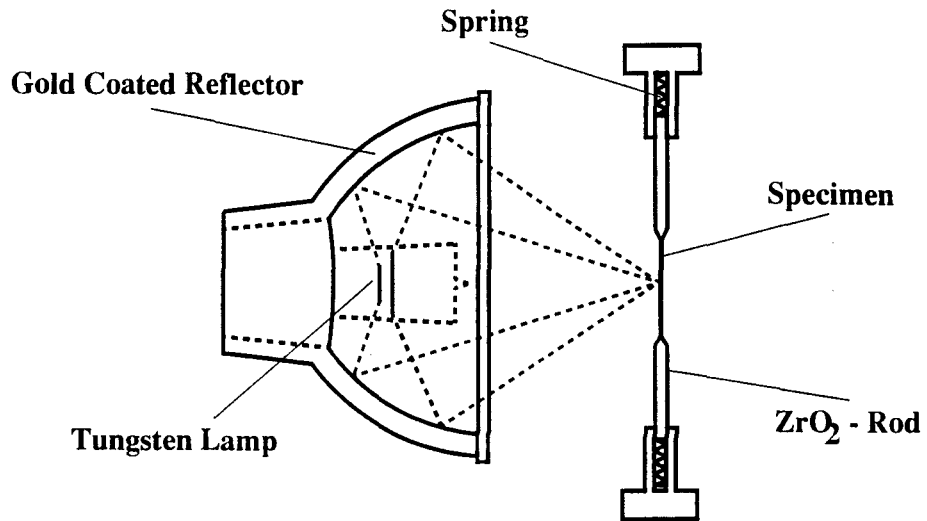
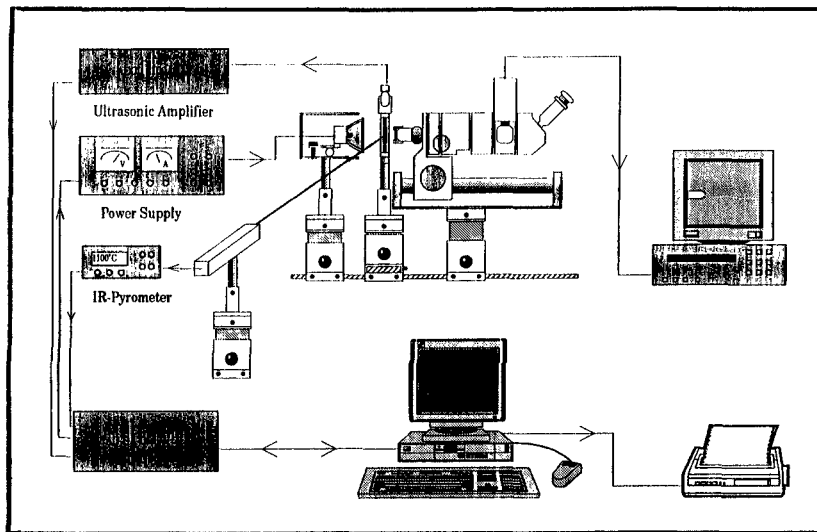Figure 1: Schematic picture of thermal shock loading cell.

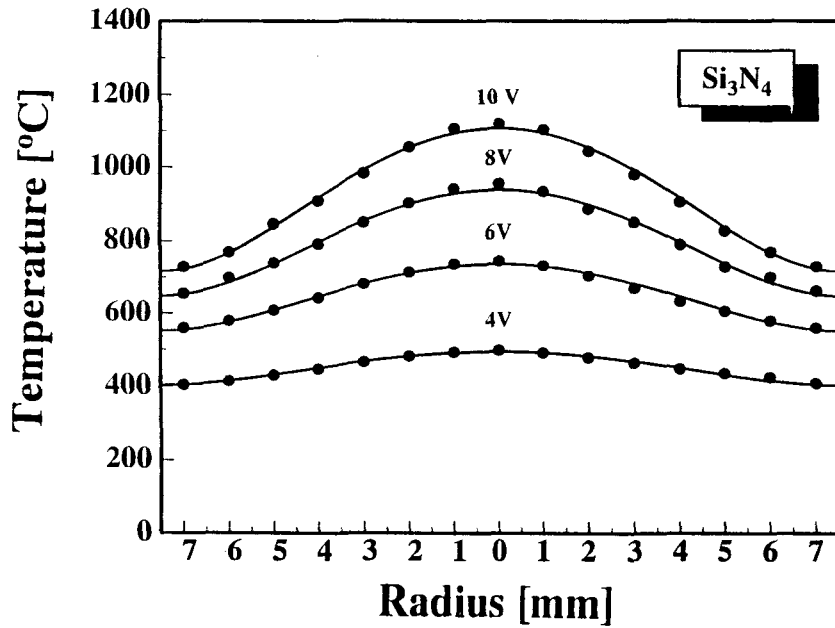Figure 2: Schematic picture of entire thermal loading system.

Figure 3: Measured static, axi-symmetrical temperature profile of Si_3N_4 for different lamp voltages.
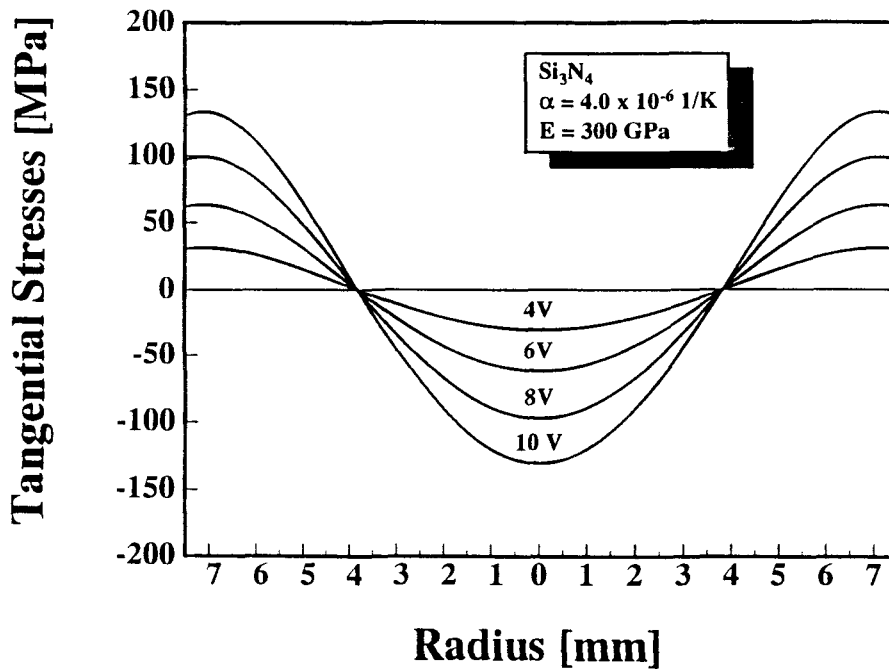

Figure 4: Calculated thermal stresses corresponding to the temperature fields of Si_3N_4 in Fig.3.

circular disk are published by Gregory. The results treat the case of a constant loading [14], quadratic loading [15] (spinning disk) and "r"-loading [16]. Applying the principle of linear superposition the stress intensity factor for a radially oriented edge crack under the hoop stresses according eq. 2 is calculated according:

$$K_I(a,t) = \alpha E \left(\frac{a}{2} \right)^{\frac{1}{2}} \left(P_2 \left(\frac{K_2(a,t)}{K_0} \right) + P_4 \left(\frac{K_4(a,t)}{K_0} \right) \right) \quad (4)$$

The details are given in the Appendix. Equation 4 delivers the crack intensity factors for the used crack geometry and temperature fields with high precision using a PC.

Figure 5 shows the calculated stress intensity factors as a function of the crack length for the measured temperature fields in Fig. 3. The maximum achievable stress intensity factors are well above the fracture toughness of Si_3N_4. The $K_I(a)$-curve shows a maximum which is typical for thermal loadings.

4. FRACTURE MECHANICS

For ceramics with a crack-length-dependent fracture toughness K_R, the beginning of crack propagation for a crack of length a which experiences a stress intensity factor K_I is determined by the conditions

$$K_I = K_R \quad (5)$$

and

$$dK_I \geq dK_R \quad (6)$$

K_R is only a function of the crack length and the differential is given by

$$dK_R = \frac{\partial K_R}{\partial a} da \quad (7)$$

On the other side the loading is time-dependent and hence

$$dK_I = \frac{\partial K_I}{\partial a} da + \frac{\partial K_I}{\partial t} dt. \quad (8)$$

By combining eq. 7 and 8 with 6 we obtain

$$\frac{\partial K_I}{\partial t} dt \geq \left(\frac{\partial K_R}{\partial a} - \frac{\partial K_I}{\partial a} \right) da \quad (9)$$

Eq. 9 allows a detailed discussion of the possible crack growth modes. At the beginning of a thermal

shock like in our experiments dK_R/dt is always positive. If

$$\left(\frac{\partial K_R}{\partial a} - \frac{\partial K_I}{\partial a} \right) \leq 0 \quad (10)$$

the so called unstable, dynamic crack propagation will occur. This means for thermal shocks and our experiments that if the initial crack lengths lies in the area where the $K_I(a)$-curve increases (short cracks) and the material exhibits a constant fracture toughness K_{IC}, equation 10 is always fulfilled and unstable, in general catastrophic crack growth occurs. For a reinforced material with increasing fracture toughness during crack extension the situation depends on the slope of the K_I-a-curve. If a very severe thermal shock occurs eq. 10 may be still fulfilled and dynamic crack propagation is initiated. If eq. 10 is not fulfilled stable crack growth will occur with a crack speed v according the identity of eq. 9:

$$v = \frac{\partial K_I}{\partial t} \left(\frac{\partial K_R}{\partial a} - \frac{\partial K_I}{\partial a} \right)^{-1} \quad (11)$$

This offers the possibility of controlled crack growth of short cracks during thermal shocks which reduces the strength of the material but avoids catastrophic failure. Equations 11 and 10 also reveal that materials with steep R-curves are advantageous.

If the crack length is in the regime where the $K_I(a)$-curve decreases the term in the bracket on the right hand side of eq. 9 is in general positive and stable crack propagation according eq. 11 occurs.

5. RESULTS AND DISCUSSION

5.1 Unstable and Stable Crack Propagation

The crack propagation experiments were performed with different initial notch lengths. In addition local thermal shocks at the notch were used to produce short, approximately 100 μm long, sharp starter cracks to study the difference between the crack growth originating from notches and sharp cracks. The results for SN84 are presented in Fig. 5. All cracks respectively notches shorter than 3.2 mm corresponding to the maximum of the $K_I(a)$-curve propagated in an unstable mode. Fig. 7 shows two video micrographs separated by 0.04 s, just before and after unstable crack growth of a sharp precrack.

Sharp cracks started at more than 1 MPa√m lower stress intensity factors revealing the influence of the 70 μm wide notch.

Figure 5 also demonstrates clearly stable crack propagation from 3.6 mm respectively 4.9 mm to 6.7 mm for Si_3N_4 in the region of negative dK_I/da. In Fig. 8 a crack propagating stably over a distance of 60 μm during a time interval of 7 s is shown. These results reveal a constant fracture toughness K_{Ic} of 4.3 MPa√m for SN84. During the measurements the crack tip passes a temperature range from 500°C to 800°C, hence the fracture toughness is measured in this temperature interval.

5.2 R-Curve behaviour

In order to study the R-curve behaviour of Si_3N_4 the wake of the sharp precracks was removed with a thin diamond blade. With this procedure it was possible to get 30 - 40 μm sharp precracks ahead of the notch. Results for the crack growth measurements with these cracks are shown in figure 6. A very steep increase of the fracture toughness from approximately 3.7 MPa√m to 5.7 MPa√m during a crack extension of approximately 50-80 μm is visible. The measurements clearly detect a non-continuous crack-extension by successive jumps in the region of increasing fracture toughness. When the plateau is reached the crack extension takes place continuously, at least within the resolution of our optical microscope. Because the R-curve is very steep it is impossible to measure it when starter precrack is longer than 50 μm. R-curve measurements at alumina have been also performed and analysed [17, 18].

5.3 Subcritical crack growth under static thermal loading

Stable crack growth was used to adjust the temperature for the beginning of SCG. Because during stable crack propagation $K_I(a(t)) = K_R$ the crack length a is a function of the applied stress intensity factor and the fracture resistance of the material,

$$a = a(K_I(t), K_R) \qquad (12)$$

and hence the crack tip temperature T_{Tip} changes according

$$T_{Tip}(t) = T(R-a(K_I(t), K_R), t) \qquad (13)$$

The crack was driven forward stably up to a certain length a_f corresponding to a certain lamp driving voltage and crack tip temperature $T_{Tip}(a_f)$, then the voltage was kept constant resulting in a stationary temperature profile. The crack extension $\Delta a = (a(t) - a_f)$ was measured as a function of time. During subcritical crack extension of ≤ 600 μm the crack tip temperature changes less than 10°C for 5 - 6 mm long cracks and therefore the crack tip temperature in the following results is given as a constant value with the above uncertainty. Results for the hot pressed Si_3N_4 are given in Figure 9 for four different crack tip temperatures. For every temperature 2 to 3 samples were measured. As can be seen in Fig. 9 the reproducibility of the results is very good. All $\Delta a(t)$ curves show a strong crack growth during the first 500 s followed by a very slow crack elongation.

The crack growth increases with increasing temperature from 790°C to 960°C. At 1040°C a strong decrease of the subcritical crack extension was measured. Because during crack extension the stress intensity factor at the crack tip is known the $\Delta a(t) \Delta a(t)$ curves can be transformed into $v(K_I)$-curves. The results corresponding to Fig. 9 are given in Fig. 10. The curves are very steep and correspond to high n-values between n = 60 at 960°C and n = 384 at 1040°C. The very slow subcritical crack growth at 1040°C is due to the softening of the viscous grain boundary phase which could be detected in the SEM. Below 1000°C the R-curve behaviour of this hot pressed Si_3N_4 is the reason of the high n values.

The fracture resistance of the material can be described by

$$K_R = K_0 + \Delta K(\Delta a) \qquad (14)$$

where K_0 denotes the base toughness of the material and ΔK describes the effect of the reinforcement mechanisms, acting during crack elongation Δa. Because the subcritical crack growth measurements were performed with very long sharp cracks the reinforcement mechanisms are already saturated and the R-curve is in the plateau region with $\Delta K(\Delta a) = \Delta K_{max}$=const. Correspondingly the stress intensity
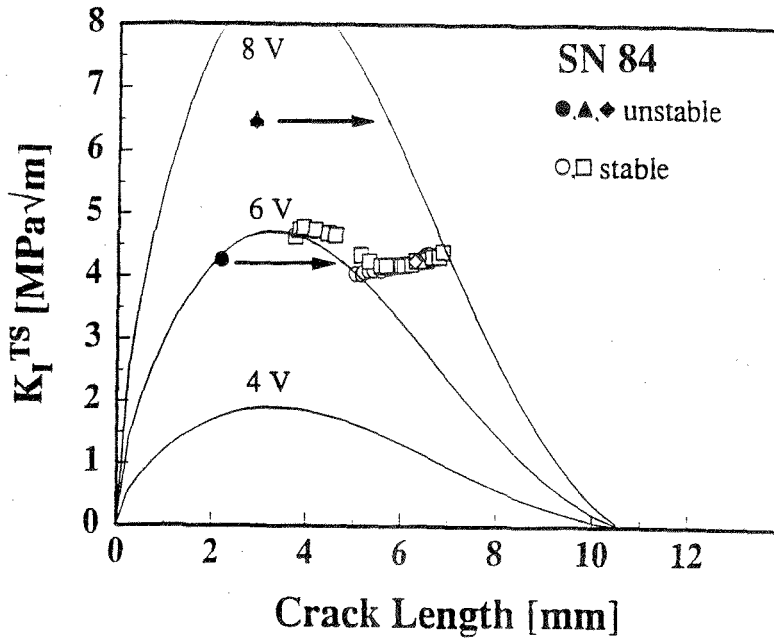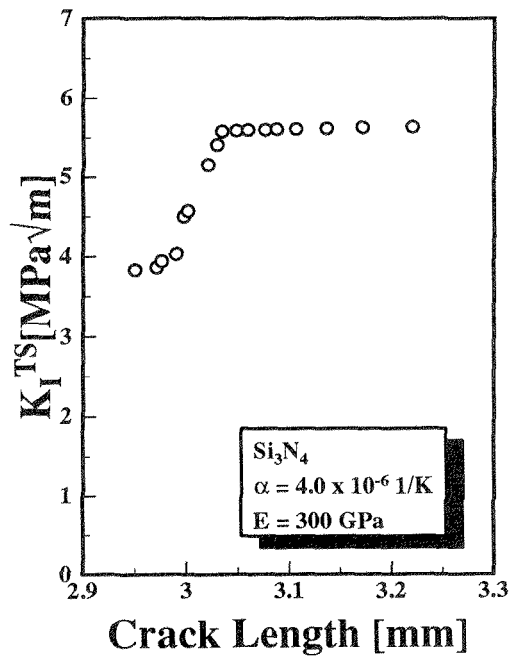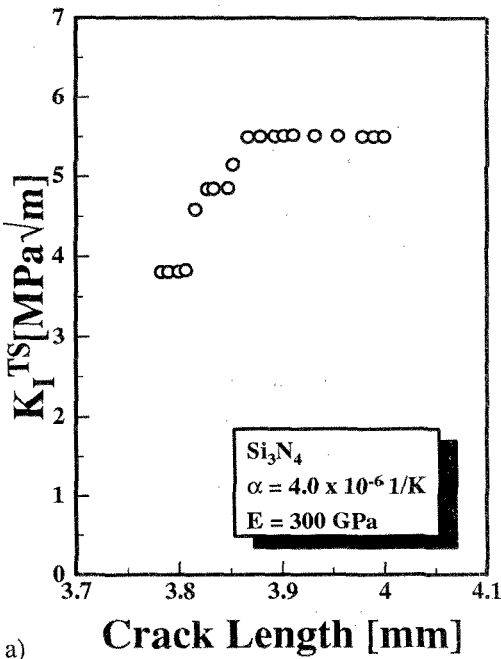
Figure 5: Stress intensity factor K_I versus crack length for a radial orientated edge crack in SN84 thermally loaded according Fig.3. "Short" cracks jump instably whereas long cracks grow stably. Specimen No. 11 and 12 were notched without a sharp starter crack.

a)

b)

Figure 6: Stable crack propagation in hot pressed $Si_3 N_4$. The fracture resistance curves a) and b) for two different notch legths exhibit very steep, short ranged R-curve behaviour. The precrack length at the notch tip was 30 µm.
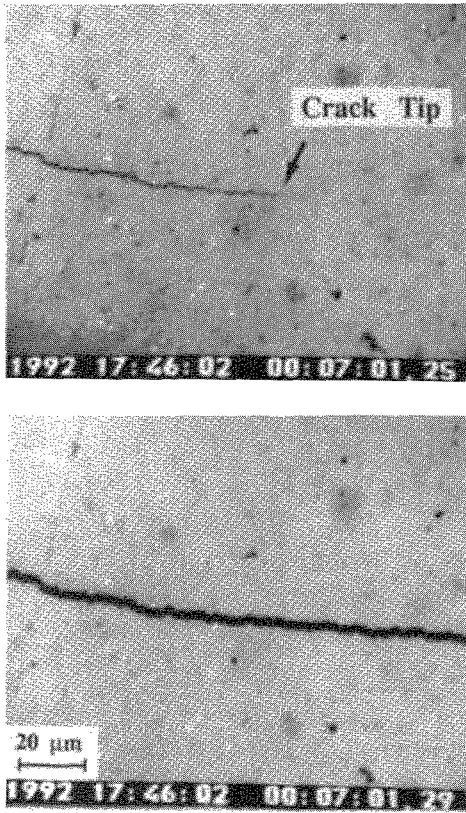
Figure 7: Unstable crack growth of a sharp crack in Si_3N_4. The pictures are taken at a 0.04s interval.

Figure 8: Stable crack growth of a sharp crack in Si_3N_4. The pictures are taken at a 7s interval.

factor at the crack tip is $K_{Tip} = K_I - \Delta K_{max}$. The measured R-curve of the hot pressed Si_3N_4 shown in Fig. 6 reveals K_0 to be 3.7 MPa$\sqrt{m}$ and $\Delta K_{max} = 2$MPa$\sqrt{m}$. Hence for the special measurement in this case the Paris law has to be formulated as follows

$$v = v_0 \left(\frac{K_I - \Delta K}{K_0} \right)^n \qquad (15)$$

where the stress intensity factor is normalised with the base toughness of the material and v_0 is the maximum velocity for SCG. Figure 11 shows the crack velocity as a function of K_{Tip}. The n-values below 1000°C are in the range between 34 and 71
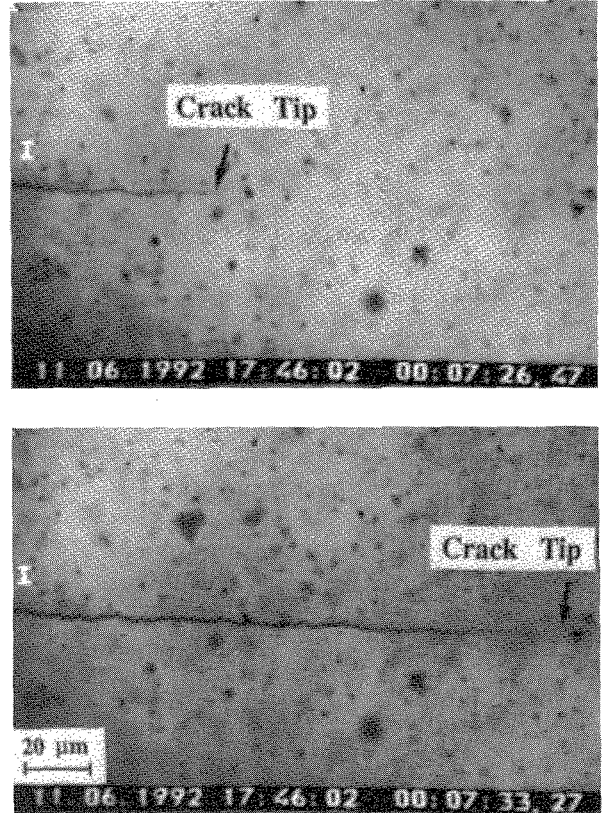
which is much lower than before where the R-curve was not taken into account.

5.4. Subcritical crack growth during thermal cycling

Thermal cycling experiments were performed similarly to the stationary loading experiments. The crack was driven forward stably up to a certain length a_f corresponding to a certain lamp driving voltage and crack tip temperature $T_{Tip}(a_f)$, then the voltage was changed sinusoidally resulting in a periodically changing temperature field on the sample after 3 to 4 cycles (Fig. 12). Crack extension was measured when periodicity in the temperature

field was reached.

Results of the measured crack extension versus time for HIPRBSN are given in Fig. 13. Up to 500 cycles corresponding to 6000s were measured with a period length of 10s. During these experiments the stress intensity factor at the crack tip varies periodically but with a decreasing maximum value $K_{max}(a)$. In order to compare the thermal cycling results with the stationary measurements the $K_{max}(a)$ was adjusted to be approximately equal to the $K_I(a)$-curve for the stationary measurements with a crack tip temperature of 920°C.

The results reveal a stronger crack growth during static loading. This has to be attributed to the different loadings. During thermal cycling only once in a period the stress intensity factor corresponding to the static loading is reached. Hence if there is no fatigue effect during thermal cycling crack growth should be slower.

6. SUMMARY

Radially oriented edge cracks in an irradiated disc were used as a model system to study the crack propagation behaviour in thermal stress fields. Unstable, stable and subcritical crack growth was detected in situ using a stereo-microscope connected to a CCD-camera. The temperature was adjusted in the range between 200°C and 1050°C. The results are as follows:

1) "Short" cracks jump unstably whereas long cracks grow in a stable mode. The separation of the two regimes is the maximum in the $K_I(a)$-curve if the material has a constant fracture toughness. The result agrees perfectly with the fracture mechanical prediction. The stable crack growth regime offers the possibility to control the crack length within some micrometer by contactless thermal loading.

2) Stable crack growth was used to measure the R-curve of hot pressed $Si_3 N_4$-ceramics. The R-curves show a very steep increase from 3.7 MPa√m to approx. 5.7 MPa√m during a crack extension of 50-80µm. The crack extension during the increase of the fracture toughness is not continuous but discrete When the fracture toughness reaches the plateau value continuous crack propagation prevails.

3) Subcritical crack growth can be detected unambiguously during stationary temperature loading and thermal cycling. These crack growth regimes can be distinguished clearly from stable crack growth.

2) Subcritical crack growth under stationary loading was evaluated in terms of $v(K_I)$-curves. The consideration of the measured R-curves explained the very slow crack velocities and made it possible to evaluate the "true" n-values of between 34 and 71 depending on the temperature.

Appendix:

With the definition
$B_2=-(3/4)a_2 R^{-2}$, $B_4=-(5/6)a_4 R^{-4}$
the coefficients P_2 and P_4 in equation 4 are:
$P_2 = (1/15) (-5 B_2 -6 B_4)$, $P_4= (4/15) B_4$.
The following table gives the normalised stress intensity factors K_2/K_0 [13] and K_4/K_0 [14] after Gregory:

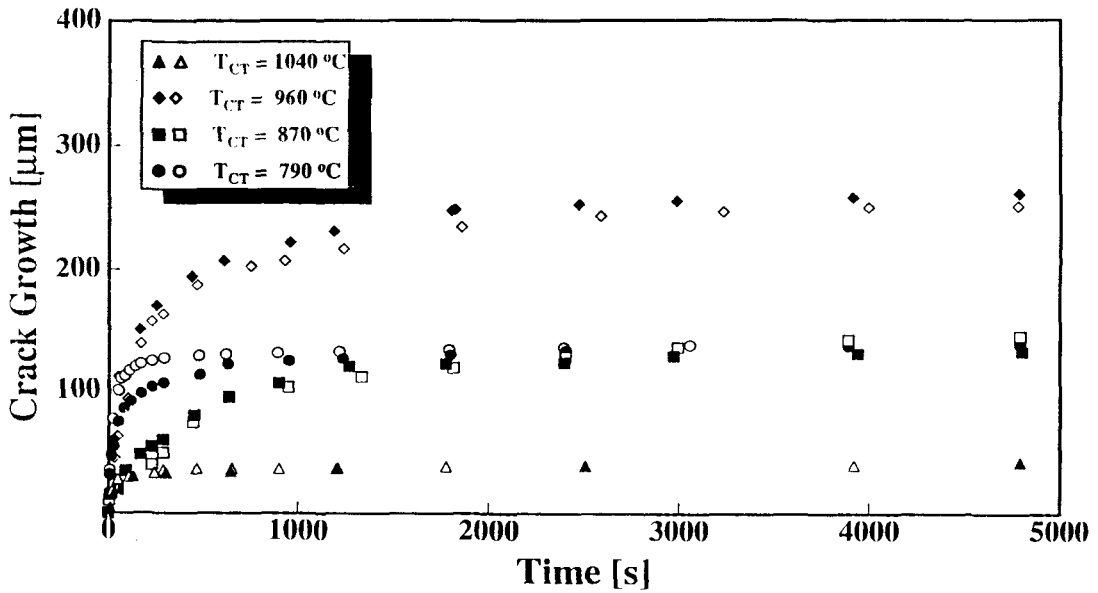| a/R	K_2/K_0	K_4/K_0
0.0	2.243	-
0.1	2.008	0.33919
0.2	1.786	0.55411
0.3	1.578	0.66839
0.4	1.382	0.70357
0.5	1.200	0.67908
0.6	1.031	0.61230
0.7	0.875	0.51849
0.8	0.732	0.41083
0.9	0.602	0.30042
1.0	0.485	0.19625
1.1	0.382	0.10524
1.2	0.291	0.03222
1.3	0.212	-.02006
1.4	0.147	-.05095
1.5	0.094	-.06184
1.6	0.054	-.05621
1.7	0.025	-.03952

Figure 9: Subcritical crack extension versus time for 4 different crack tip temperatures of hot pressed Si_3N_4 .
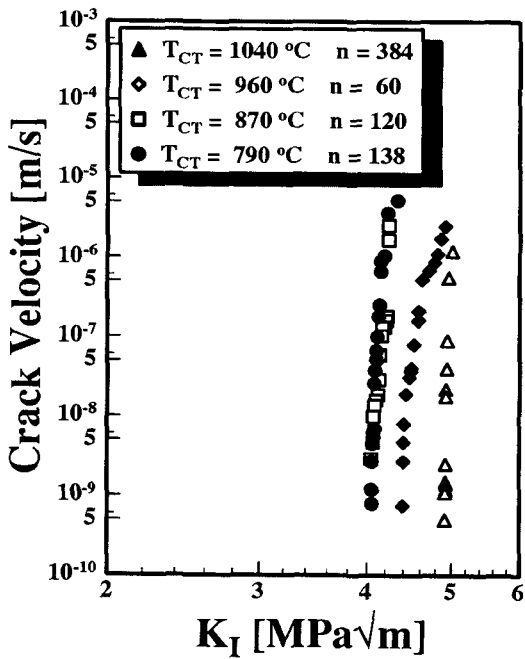

Figure 10: Subcritical crack velocity as a function of the applied stress intensity factor K_I corresponding to the results of Fig. 9.

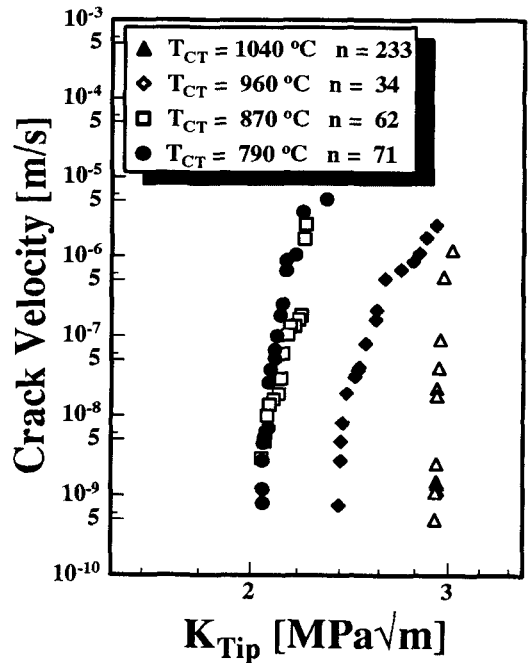Figure 11: Subcritical crack velocity as a function of the stress intensity factor at the crack tip, $K_{Tip}=K_I-\Delta K_{max}$, corresponding to the results of Fig. 9.
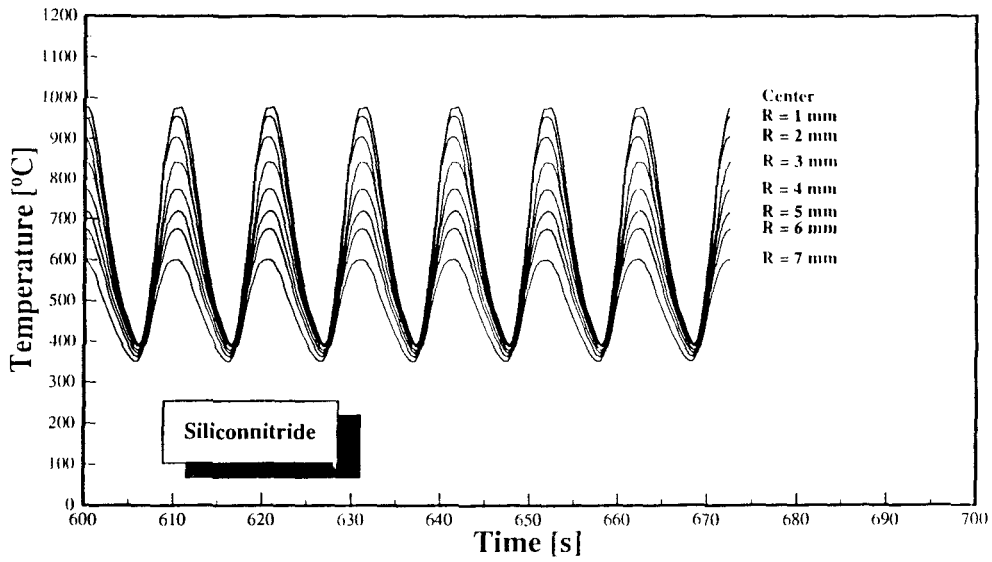
Figure 12: Periodically variing temperature field during thermal cycling of HIPRBSN.

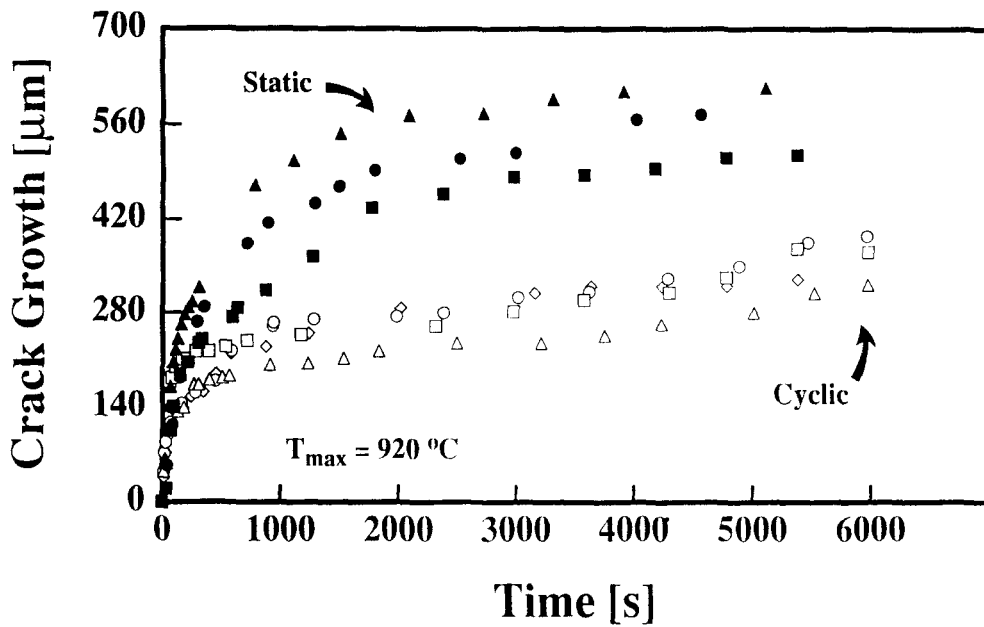

Figure 13: Subcritical crack extension versus time for thermal cycling of HIPRBSN.with the temperature field of Fig. 12. For comparison the corresponding crack extension for stationary loading with a crack tip temperature of 920°C is also shown.

1.8	0.008	-.01909
1.9	0.001	-.00364

The results of the above table were fitted with high order polynomials in order to facilitate the numerical calculations.

References

[1] R. Badaliance, D.A. Krohn, D.P.H. Hasselman, "Effect of Slow Crack Growth on the Thermal-Stress Resistance of an Na^2O-CaO-SiO^2 Glass", J. Am. Cer. Soc. 57 432 (1974)

[2] S. Sato, K. Sato, Y. Imamura, J. Kon, "Determination of the Thermal Shock Resistance of Graphite by Arc Discharge Heating", Carbon 13 309 (1975)

[3] H.S. Starrett, A.D. Cull, G.R. Irwin,"Application of Fracture Mechanics to the Thermostructural Failure of Graphite", pp. 86-108 in Cracks and Fracture, ASTM STP 601, American Society for Testing and Materials, 1976,

[4] D. Stahn, F. Kerkhof, "Bruchgefährdung von thermoschockbelasteten Glasscheiben", Glastechnische Berichte 50 121-128 (1977)

[5] A.F. Emery, "Thermal Stress Fracture in Elastic-Brittle Materials, pp. 95-121 in Thermal Stresses in Severe Environments, edited by D.P.H. Hasselman and R.A. Heller, Plenum Press, New York, 1980

[6] A.F. Emery, A.S. Kobayashi, "Transient Stress Intensity Factors for Edge and Corner Cracks in Quench-Test Specimens", J. Am. Cer. Soc. 63 410-415 (1980)

[7] C. Schubert , H.-A. Bahr, H.-J. Weiss,"Crack Propagation and Thermal Shock Damage in Graphite Disks Heated by Moving Electron Beam", Carbon 24, 21-28 (1986)

[8] K. Keller, "Theoretische und experimentelle Untersuchungen zur Thermoermüdung keramischer Werkstoffe", Dissertation, University of Karlsruhe, 1989

[9] F. Sudreau, "Methodes d'Analyse et de Simulation de la Fatigue Thermique de Ceramiques Thermomecaniques", Dissertation, L'Institut Natational des Sciences Appliques de Lyon, 1992

[10] G.A. Schneider, G. Petzow, "Thermal Shock Testing of Ceramics - A New Testing Method", J. Am. Cer. Soc. 74 [1] 98-102 (1991)

[11] G.A. Schneider, F. Magerl, I. Hahn, G. Petzow, "In Situ Observations of Unstable and Stable Crack Propagation and R-Curve Behavior in Thermally Loaded Discs" in Thermal Shock and Thermal Fatigue Behavior of Advanced Ceramics, ed. by G.A. Schneider and G. Petzow, NATO ASI Series, Series E: Applied Sciences - Vol. 241, 1993 Kluwer Academic Publishers, Dordrecht, The Netherlands, 229-244

[12] B.A. Boley and J.H. Weiner, Theory of Thermal Stresses, R.E. Krieger, Malabar, FL, 1985

[13] G. Kirchhoff, "Thermal Shock Fracture by Laser Irradiation", in Thermal Shock and Thermal Fatigue Behavior of Advanced Ceramics, ed. by G.A. Schneider and G. Petzow, NATO ASI Series, Series E: Applied Sciences - Vol. 241, 1993 Kluwer Academic Publishers, Dordrecht, The Netherlands, 245-252

[14] R.D. Gregory, "A circular disc containing a radial edge crack opened by a constant internal pressure", Math. Proc. Camb. Phil. Soc. 81 497-521 (1977)

[15] R.D. Gregory, "The spinning circular disc with a radial edge crack; an exact solution", International Journal of Fracture 41 39-50 (1989)

[16] R.D. Gregory, private communication

[17] I. Hahn, G.A. Schneider, G. Petzow, "R-Curve Behaviour of Alumina under Thermal Stresses", submitted to J. Am. Cer. Soc.

[18] H.-A. Bahr, T. Fett, I. Hahn, D. Munz,, I. Pflugbeil, "Fracture Mechanics Treatment of Thermal Shock and the Effect of Bridging Stresses", in Thermal Shock and Thermal Fatigue Behavior of Advanced Ceramics, ed. by G.A. Schneider and G. Petzow, NATO ASI Series, Series E: Applied Sciences - Vol. 241, 1993 Kluwer Academic Publishers, Dordrecht, The Netherlands, 105-118

Emeritus Prof. Dr. Dr. h.c. mult
Günter Petzow